Supplementary Materials

Sustainable PH_3 Purification over MOF-Derived Ce-Doped CuO Materials: Enhanced Performance and Closed-Loop Resource Recovery

Haoyang Yi [1, 2], Kai Li [2, 3], Bo Li [2], Chi Wang [1]*, Kunlin Li [2, 3]*, Ping Ning [2, 3]

[1] Faculty of Chemical Engineering, Kunming University of Science and Technology, Kunming 650500, PR China

[2] Faculty of Environmental Science and Engineering, Kunming University of Science and Technology, Kunming 650500, PR China

[3] National-Regional Engineering Center for Recovery of Waste Gases from Metallurgical and Chemical Industries, Kunming University of Science and Technology, Kunming 650500, PR China

*Corresponding Authors,

E-mail addresses: wangchikg@163.com (Chi Wang), lkl@kust.edu.cn (Kunlin Li).

Table of contents

Supplementary S1: Characterization methods **2**

Supplementary Figures **4**

Figure S1. (a) N_2 adsorption isotherm of different adsorbents, Pore size distribution curves of (b) MOF-199, (c) MOF-derived CuO, (d) $Cu_1Ce_{0.2}O$ 4
Figure S2. XRD pattern of $Cu_1Ce_{0.14}O$, $Cu_1Ce_{0.2}O$, Cu_1Ce_1O. 5
Figure S3. The PH_3 adsorption–oxidation performance of $Cu_1Ce_{0.2}O$ prepared at different calcination temperatures 6
Figure S4. The PH_3 adsorption–oxidation performance of $Cu_1Ce_{0.2}O$ at varying PH_3 concentrations 7
Figure S5. The PH_3 adsorption–oxidation performance of $Cu_1Ce_{0.2}O$ at varying humidity 8
Figure S6. The PH_3 adsorption–oxidation performance of $Cu_1Ce_{0.2}O$ at varying oxygen levels 9
Figure S7. TEM of exhausted adsorbent 10
Figure S8. Effect of RhB catalytic degradation under visible light or dark conditions of exhausted adsorbent 10
Figure S9. XRD pattern of exhausted adsorbent after RhB catalytic degradation 12
Figure S10. Cyclic performance of the exhausted adsorbent in the catalytic degradation of RhB under visible light conditions 13

Supplementary S1: Characterization methods

In order to explore the physical and chemical properties of adsorbents, various characterization and analysis techniques wre usually used to detect them. SEM and EDS were used to analyze the micromorphology and element distribution of each adsorbent. N_2 adsorption-desorption isotherms was used to detect the specific surface area and pore size distribution of the adsorbent. TEM was used to analyze the surface lattices and special interfaces of adsorbents. XRD was used to analyze the crystal phase composition and surface crystal structure of the adsorbent. TG was used to analyze the effect of high temperature roasting on the adsorbent. XPS was used to determine the element content, chemical valence and chemical composition of the adsorbent surface. EPR was used to analyze the effect of the modification on the surface oxygen vacancy of the adsorbent. H_2-TPR was used to analyze the redox properties of adsorbents. CO_2-TPD was used to determine the number and strength of the basic sites of the adsorbent. The following is the specific information of each characterization method.

SEM: A small amount of sample is directly attached to the conductive adhesive and then gold-coated using a Quorum SC 7620 sputtering coating instrument for 45 seconds at a current of 10 mA. The morphology and energy dispersive spectroscopy mapping tests are performed using a TESCAN MIRA LMS scanning electron microscope. During testing, the acceleration voltage is 3 kV, and the energy dispersive spectroscopy mapping acceleration voltage is

15 kV. The detector used is an SE2 secondary electron detector.

N_2 adsorption-desorption isotherms: The samples were pretreated under 300 ℃ for 3 h, and then the nitrogen adsorption-desorption isotherm of the samples was measured at 77 K by a physical adsorption instrument (model BELSORP-max, Mecabier, Japan). The specific surface area and pore size distribution of the samples were calculated from the nitrogen adsorption-desorption isotherm.

TEM: A part of the sample was dispersed into an ethanol solution for ultrasonic treatment. Then, a few drops of the dispersed liquid were added drop by drop to the copper wire, and after drying, the morphology (high resolution) was photographed using a transmission electron microscope (model JEOL JEM-F200). The accelerating voltage used in the test was 200 kV, and the energy dispersive spectrometer model was JED-2300T.

XRD: The test instrument is X-ray diffractometer (Ultima IV, Japan Riken Corporation). The wavelength λ of Cu-Ka ray is 0.15406 nm, the operating voltage is 40 kV, the operating current is 40 mA, the scanning speed is $5° \cdot min^{-1}$, and the scanning range is 5-90°. The test data are analyzed and processed by MDI Jade.

TG: The sample was placed on the precision balance inside the instrument and heated from room temperature to 1000 ℃ at a rate of $5\ ℃ \cdot min^{-1}$. The change of sample mass was detected by thermogravimetric analyzer (model TGA-2, Mettler Toledo, USA & Switzerland).

XPS: After pressing an appropriate amount of sample into a sheet, place it on the sample tray and insert the sample into the sample chamber of the Thermo Scientific K-Alpha XPS instrument. When the pressure in the sample chamber is less than 2.0×10^{-7} mbar, send the sample to the analysis chamber. The spot size is 400 μm, with a working voltage of 12 kV and filament current of 6 mA; the full-spectrum scan energy range is 150 eV with a step size of 1 eV; the narrow-spectrum scan energy range is 50 eV with a step size of 0.1 eV. The raw data obtained is processed for peak decomposition and fitting using Avantage.

H_2-TPR: Place the sample in the reaction tube and heat it to 300 ℃ under a high-purity argon atmosphere for 1 h. After cooling to 50 ℃, introduce a mixed gas of H_2 and Ar (with 10% H_2 content), and increase the temperature from 50 ℃ to 800 ℃. Use a chemical adsorption instrument (Auto Chem1II 2920, Micromeritics, USA) to measure the consumption of H_2.

CO_2-TPD: Place the sample in the reaction tube and heat it to 300 ℃ for drying pretreatment. After purging with a He gas flow for 1 h, cool it to 50 ℃, then introduce a mixed gas of CO_2 and He until saturation, followed by another 1 h of He gas purging. Finally, heat it to 800 ℃ and use a chemical adsorption instrument (Auto Chem1II 2920, Micromeritics, USA) to measure the CO_2 desorption amount.

Supplementary Figures

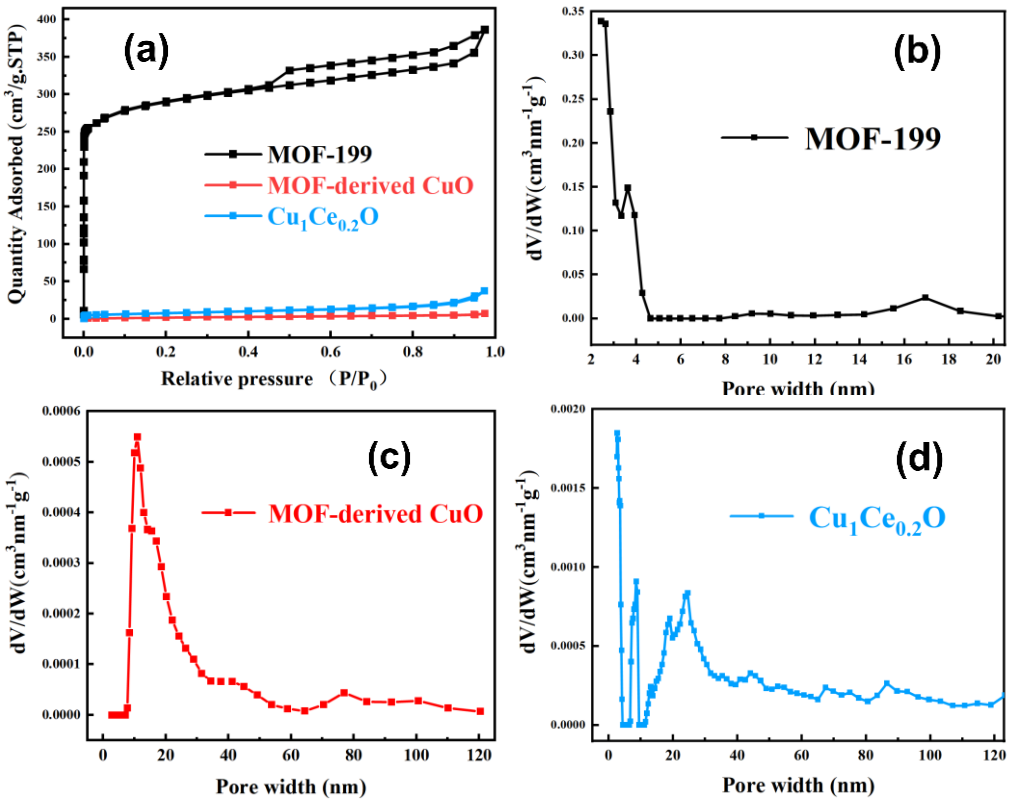


Figure S1. (a) N_2 adsorption isotherm of different adsorbents, Pore size distribution curves of (b) MOF-199, (c) MOF-derived CuO, (d) $Cu_1Ce_{0.2}O$.

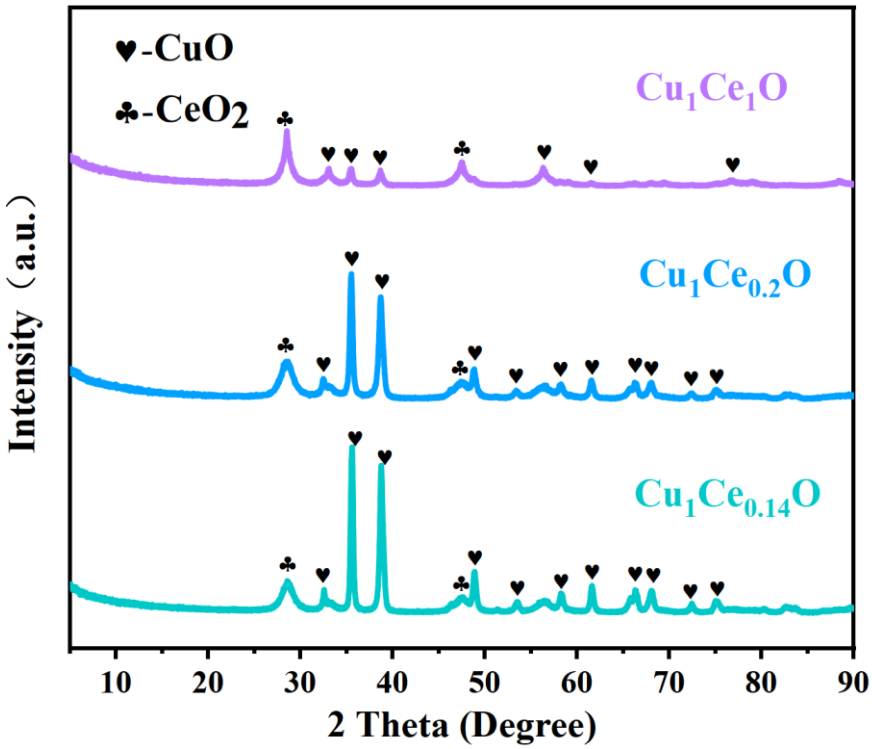


Figure S2. XRD pattern of $Cu_1Ce_{0.14}O$, $Cu_1Ce_{0.2}O$, Cu_1Ce_1O.

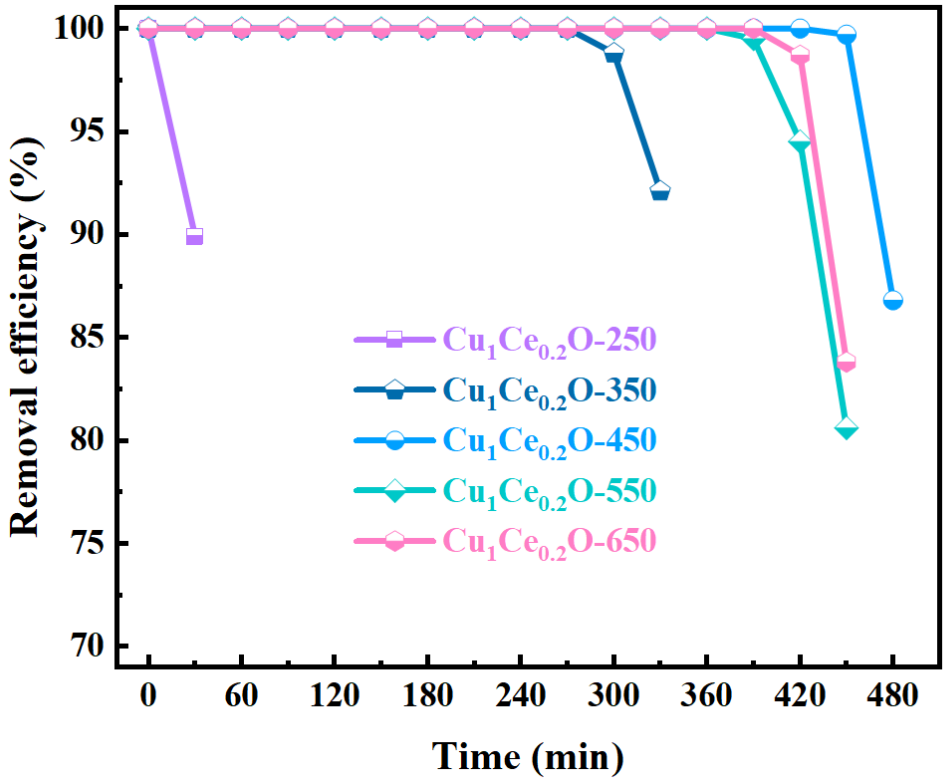


Figure S3. The PH_3 adsorption–oxidation performance of $Cu_1Ce_{0.2}O$ prepared at different calcination temperatures.

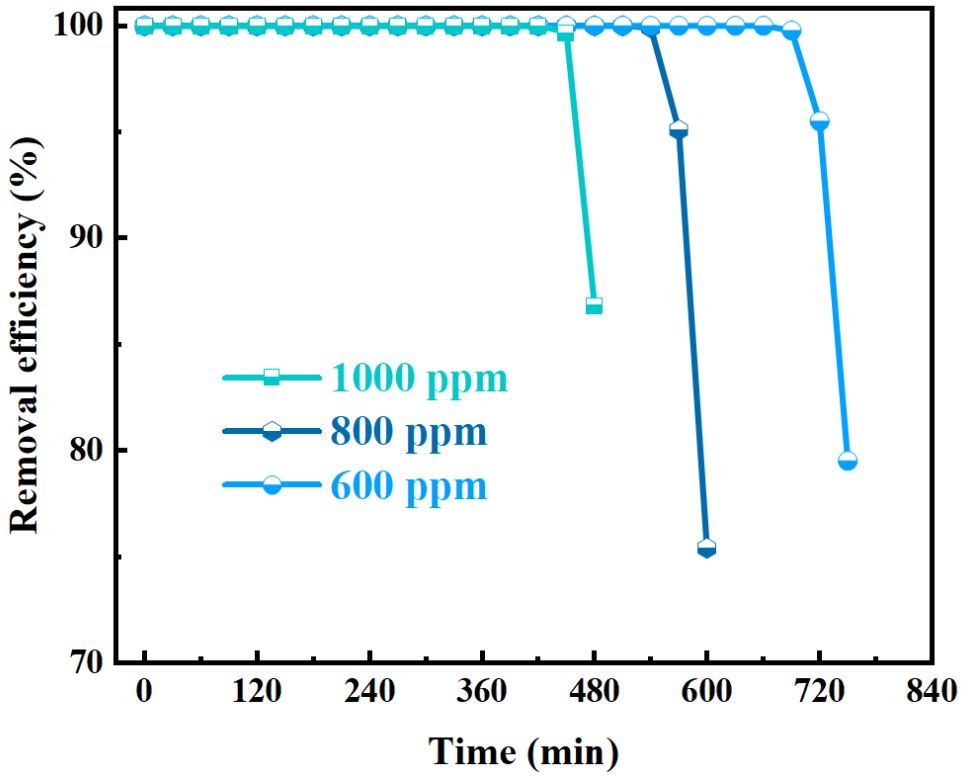


Figure S4. The PH_3 adsorption–oxidation performance of $Cu_1Ce_{0.2}O$ at varying PH_3 concentrations.

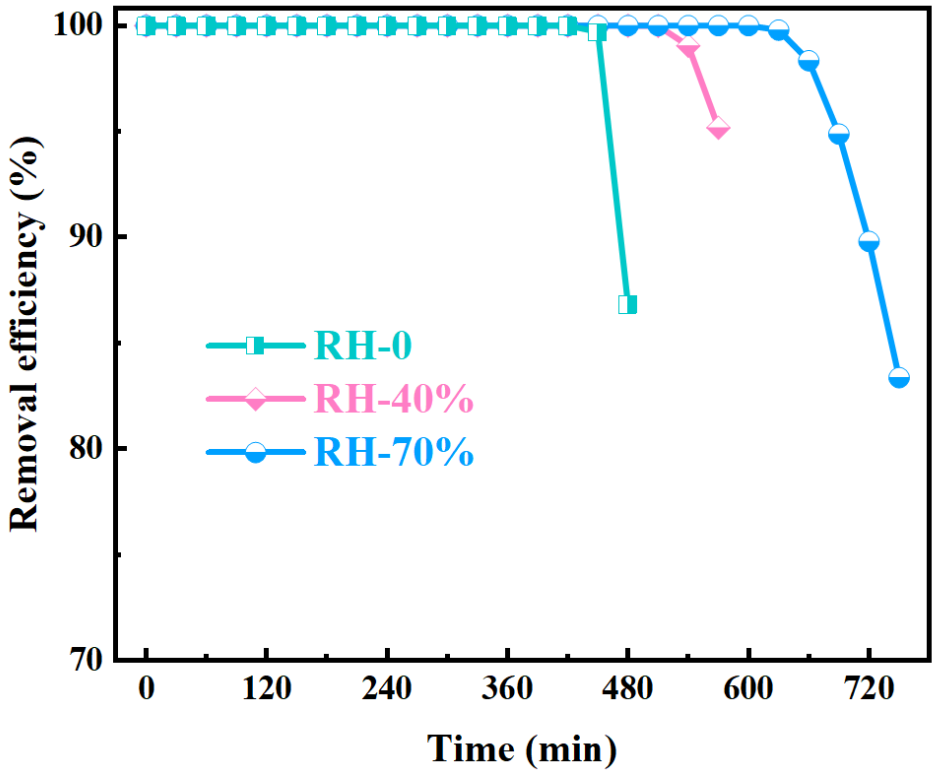


Figure S5. The PH_3 adsorption–oxidation performance of $Cu_1Ce_{0.2}O$ at varying humidity.

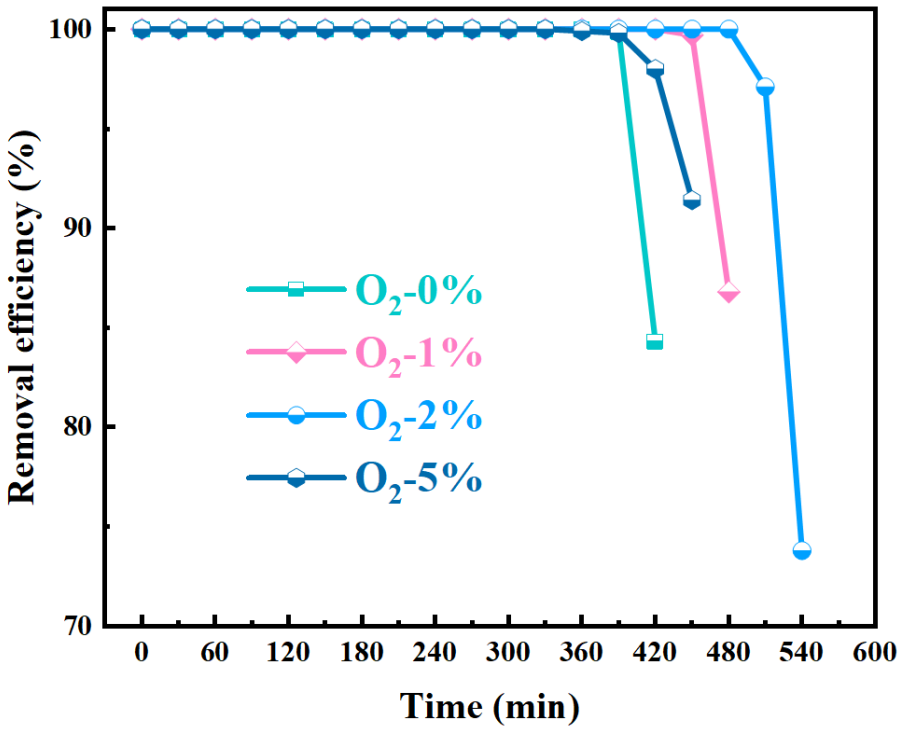


Figure S6. The PH_3 adsorption–oxidation performance of $Cu_1Ce_{0.2}O$ at varying oxygen levels.

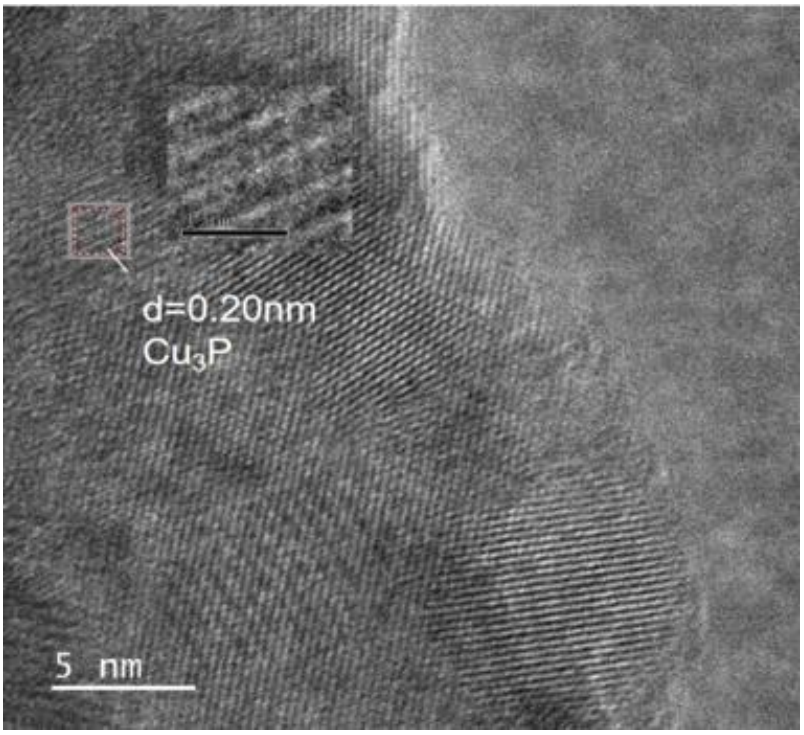


Figure S7. TEM of exhausted adsorbent.

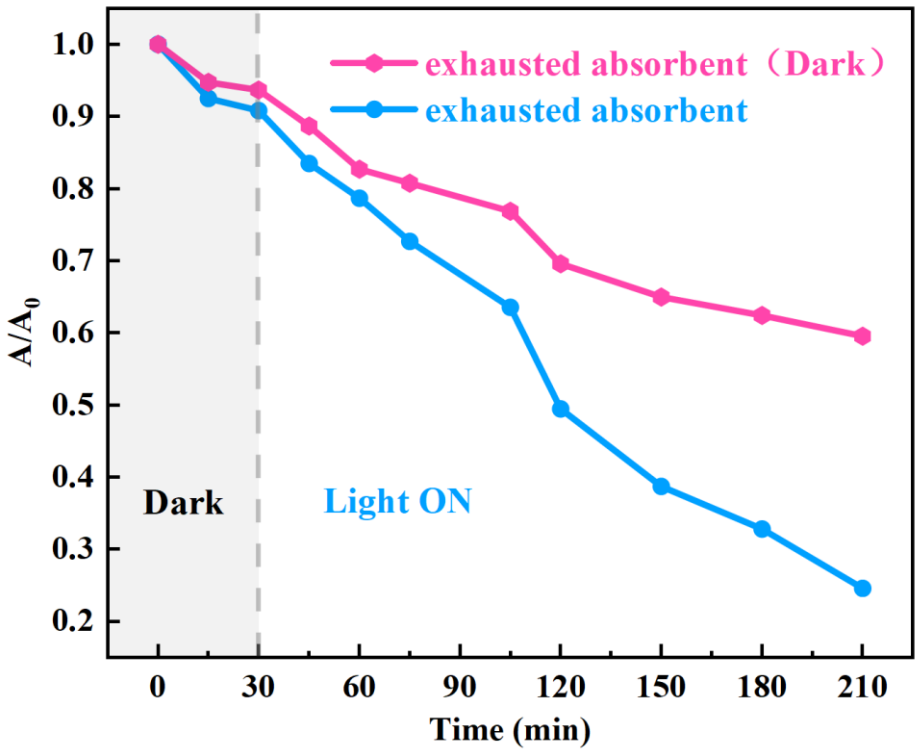


Figure S8. Effect of RhB catalytic degradation under visible light or dark conditions of exhausted adsorbent.

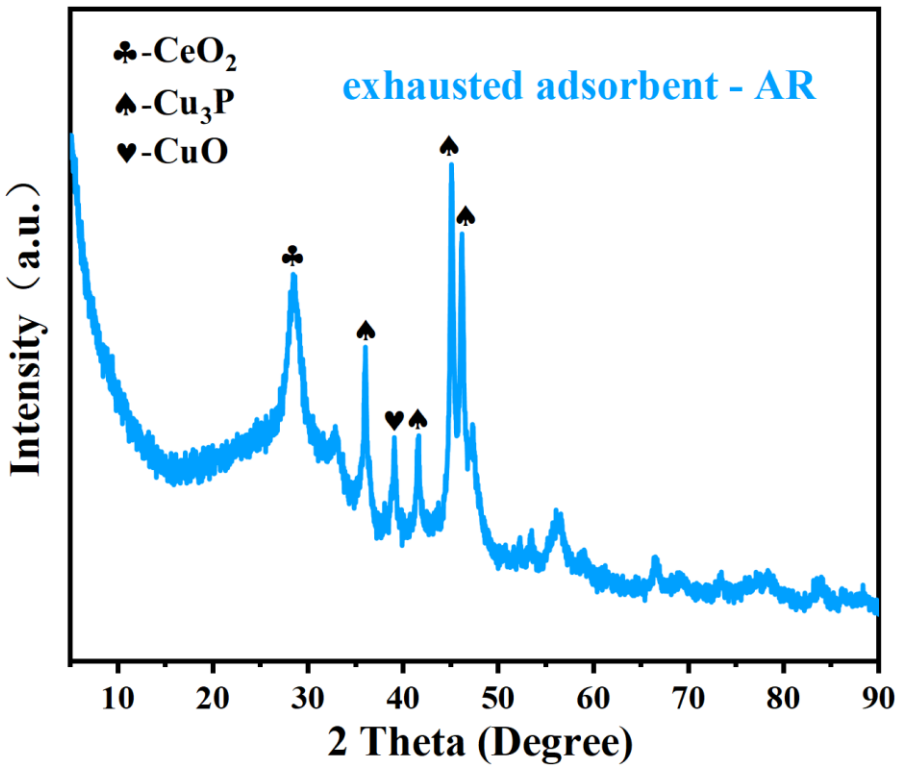


Figure S9. XRD pattern of exhausted adsorbent after RhB catalytic degradation.

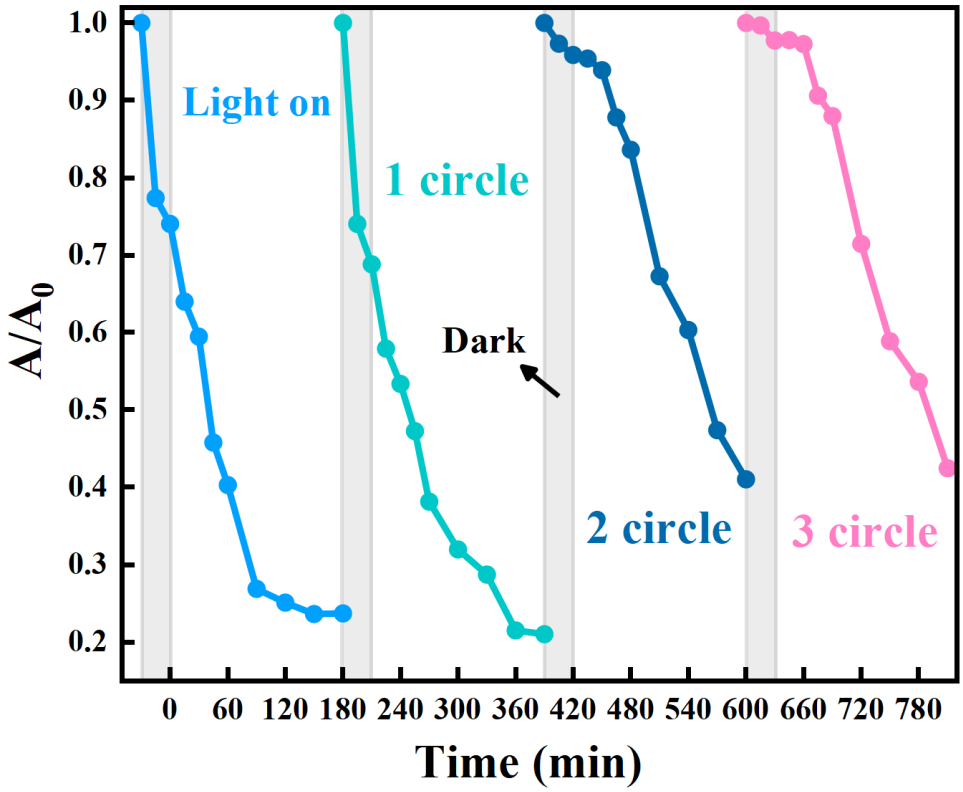


Figure S10. Cyclic performance of the exhausted adsorbent in the catalytic degradation of RhB under visible light conditions.